

Description and modelling of the multi-axial stiffness degradation in fatigue loaded NCFs under sequence loading

F. Schmidt, S. Adden, E. Möhle and P. Horst

Institute of Aircraft Design and Lightweight Structures, TU Braunschweig
Hermann-Blenk-Straße 35, 38106 Braunschweig

ABSTRACT

In the current paper experimental and analytical results of research on fatigue loaded NCFs under sequence loads, which mean a change from pure shear load to pure compressive/tension load after several life cycles, are given. After a short introduction the specimens and the destructive and non-destructive test-procedure is described. In addition to the experimental tests an analytical modelling approach is presented. The approach is based on a cracked finite-element RVE and uses crack densities measured in the experiments. The influence of cracks on the stiffness degradation of NCFs is established by the model. The application of the model to fatigue sequence loaded tube specimens is shown and the results of the modelling approach are compared with the experimental results.

1. INTRODUCTION

Non-Crimp-Fabrics (NCFs) are complex materials compared to unstitched laminates. Their laminate lay-up always includes different sub-ply with different orientations, which are held together by a stitching yarn. Therefore the need for NCFs only arises, when materials with complex fibre orientations and therefore complex loading conditions are used. Due to the stitching a complex lay-up can be realized with just a few NCFs, where cost-savings in production processes are possible. Disadvantages of the stitching process are the local inhomogenities and the misalignment of fibres in the material. Therefore several research programs with NCFs were executed in the past. After comparison different glass-fibre and carbon-fibre NCFs in compression and tensile tests Bibo et al. [1] came to the conclusion that different stitching parameters have an influence on the compression strength whereas the influence on the tension strength is very low. Other works of Hogg et al. [2] show that the NCFs have superior mechanical properties by comparing NCFs to woven fabrics. This statement is based on experimental tension and flexure tests. Carvelli et al. [3,4] declared that the NCF's behaviour widely agrees with the behaviour of non-stitched laminates. Looking at the modelling approach this is an important conclusion.

One objective of this work is to characterize the behaviour of NCFs by experimental tests with bi-axial sequence fatigue loads. Sequence loads mean a change from pure shear load to pure compressive/tension load after several life cycles. Bi-axial loads mean a combination of tension/compression and torsion with arbitrary load ratios. Under fatigue load each sub-ply of NCFs will be loaded by transverse and shear loads, which will cause cracking in the matrix of this ply. Cracking leads to a local stiffness reduction of the ply, which again will lead to load redistributions in the laminate and a global stiffness reduction. This effect will be shown and additionally a modelling part based on a representative volume element (RVE) will be presented. The theoretical approach is capable of modelling the stiffness reduction due to cracks in arbitrary NCFs for given damage states.

2. EXPERIMENTS

Especially bi-axial and sequence fatigue loading tube specimens and a servohydraulic tension-torsion machine, which allows applying tensional as well as torsional loading, are required. For the crack-characterization non destructive tests with light microscope are conducted.

2.1 Tube specimen

The tube specimens used in the experiments are made of glass-fibre non-crimped-fabrics and the common resin/hardener combination L135i/H137/H134, which is used in the wind-energy industry. The NCF, provided by SAERTEX^R, consists of 4 sub-layers with approximately 50% of the mass per unit area in 0° direction, the +45°- and -45°-layers have with approximately 23% of the mass per unit area the same size and the layer in 90° direction possesses approximately 4% of the mass per unit area. Table 1 shows the special lay-up.

SAERTEX ^R V92402-01310-01270-000000	
Orientation	Mass per unit area
0°	638 g/m ²
-45°	301 g/m ²
90°	63 g/m ²
45°	301 g/m ²

Table 1: Lay-up of the used NCF

The final laminate consists of two layers of NCF and is fabricated using resin transfer moulding (RTM). It is important to mention that the specimens are manufactured in a way that the 0° direction of the NCF is identical to the axial direction of the tube specimen. Figure 1 shows one tube specimen. The bonded steel inserts and the doubler for enforcing the ends of the tube specimen are required. Both of them prevent failure caused by the fixing pressure of the testing machine.

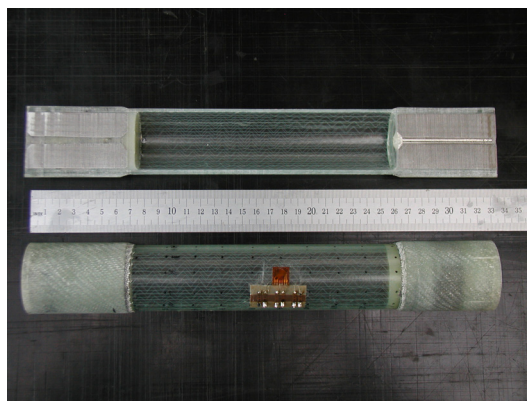


Figure 1: Tube specimen for experiments of bi-axial and sequence fatigue loads

The advantages of the tube specimen are the possibility to apply bi-axial and sequence loads (axial and torsional loads) and the minimization of the so called free-edge-effect, which occurs under fatigue loading by using coupon specimens.

Due to the special lay-up of the material and the variation of loads high intra- and inter-laminar stresses occur. The magnitude depends on the loading conditions and the percentage of fibers, which are in different layers and not orientated in the loading direction. The results are cracks in several layers and in turn a decrease of the material stiffness. In this paper the

relationship between the three parameters crack density, loading cycles and stiffness will be shown by experimental tests and used as input into a modelling approach.

2.2 Bi-axial and sequence fatigue loads

The experimental tests were accomplished by a tension torsion machine (MTS 319.25). The circular clamping of the machine enables the test of tube specimens. All fatigue tests were performed in a force-controlled manner using a stress ratio of $R = -1$. By using different ratios of tension force and torsional moments different bi-axial and sequence loading ratios are possible to apply by either turning the upper end of the specimen against the lower end (shear), by moving the upper end axial against the lower end (axial tension) or by combination and sequence of both. For sequence fatigue loads the tube specimens were alternately loaded with tension/compressive forces and torsion moments. These changes of loads were performed after 5000 and 10000 loading cycles. Another parameter of the sequence fatigue loading tests was that some tube specimens were at first loaded with tension/compressive forces and the other ones were at first loaded with torsion moments.

In order to calculate the material stiffness, the fatigue tests were divided into characterization and fatigue damage steps. The characterization steps are quasi-static tests by using a tension force to calculate the Young's Modulus and by using a torsion moment to calculate the Shear Modulus of the tube specimen. The loads of the characterization steps were considerably smaller than the applied load in fatigue steps and chosen in a way that no further damage is introduced. Then the fatigue steps were performed in order to introduce the damages. Figure 2 shows this typical loading sequence.

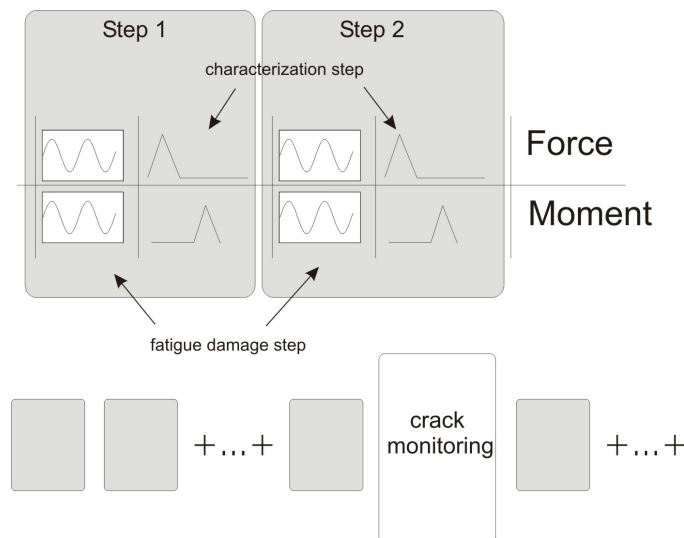


Figure 2: Typical experimental process with fatigue damage and characterization steps

2.3. Crack Monitoring

Crack Monitoring is required to determine the crack density, which is one of the most interesting parameters for describing material behaviour. The advantage of the material used here is the transparency, because the refraction index of fibre and resin is almost similar. Therefore the cracks can be observed by using a light microscope. At the beginning of the experiments ten areas of the specimens were marked and monitored after several fatigue damage steps (shows in Figure 2). For using the microscope the fatigue damage steps have to be stopped and the specimen was taken out of the machine. In all photos of each area after several fatigue steps the cracks were counted and based on the geometries the averaged crack density δ was computed.

3. MODELLING APPROACH

The aim of the modelling approach is the description of the stiffness degradation of NCFs with arbitrary layers. The basis of the approach is a finite element representative volume element (using MSC.Patran and Abaqus), which computes the stiffness degradation of one layer separately dependent on a damage parameter D (D is equal to the product of crack density δ and thickness t). Adden et al. [6] describes the motivation (determine constitutive relations for a crack ply under arbitrary geometrical conditions), the possible application and the detail approach of the RVE. The next steps of his work are comparable to the current works. Figure 3 visualizes a schematic plan of necessary steps of the modelling approach in order to get the stiffness degradation of the NCFs with the base of single-ply RVE model.

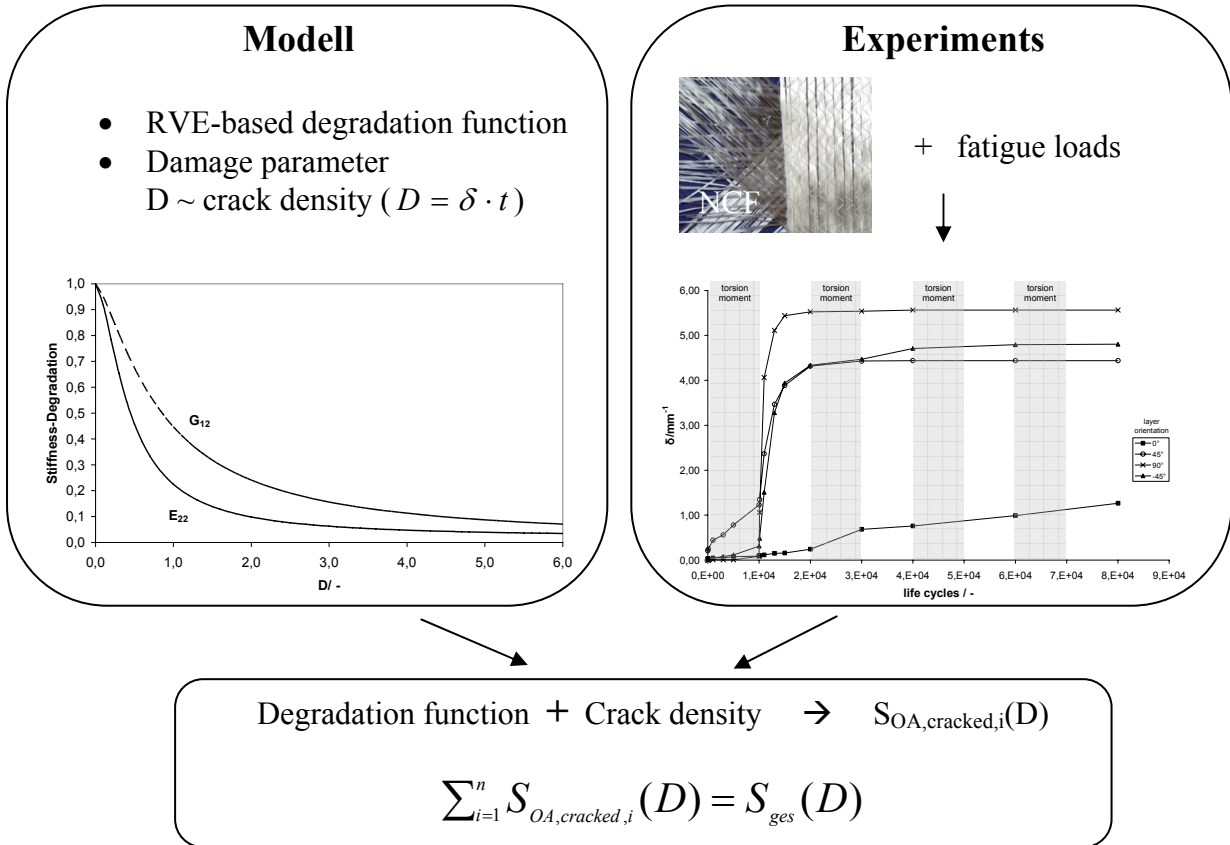


Figure 3: Plan of procedures of the modelling approach

The damage parameter D of the modelling approach is directly linked to the crack densities measured for each layer during the experimental tests. So it is possible to calculate the stiffness matrix $S_{OA,cracked,i}(D)$ for each single cracked ply. In order to compare the modelling approach to the experimental tests the last necessary step is to calculate the laminate stiffness by using the classical laminate theory. The transferability from arbitrary layers to the NCFs does not seem reasonable at first sight because the NCF consists of stitching yarn, which should influence the stiffness of the material. As mentioned in the introduction several works show that NCFs and unstitched materials are comparable regarding the description of the stiffness. Adden et al. [5,6] shows the translation of this model approach to arbitrary layers of NCFs for uni- and bi-axial fatigue loads. The focus of this paper is the application of this modelling approach to compute the stiffness degradation due to sequence fatigue loads and arbitrary layers of NCFs.

4. EXPERIMENTAL RESULTS

As mentioned above, the Young's and the Shear Modulus were calculated with characterization steps and so the decreases of these depending on the loading cycles are determinable. Figure 4 shows experimental degradation results for a specimen under sequence fatigue with alternating shear and compressive/tension loads.

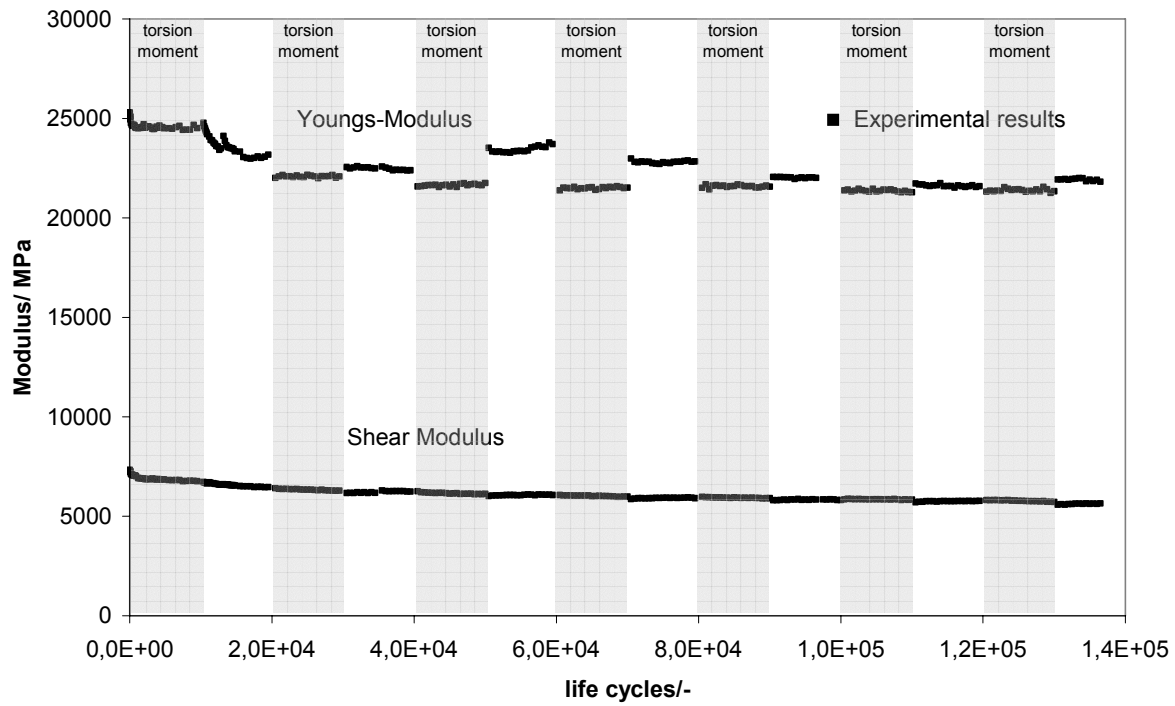


Figure 4: Experimental degradation results of Young's and Shear Modulus for a specimen under sequence fatigue with alternating shear and compressive/tension load

During the first shear loading block up to 10000 life cycles a slow, almost linear decrease of the Young's and the Shear Modulus can be seen. In the next loading phase and under the first compressive/tension loading block a typical rapid decrease of the Young's Modulus is detected. In this phase the Shear Modulus still shows a lower decrease than the Young's Modulus. After the first compressive/tension loading block and under the sequence fatigue loads a variation of the Young's Modulus is measured. These steps between both parts of the slopes of the Young's Modulus after a shear load phase and in the next compressive/tension phase is caused by the measurement of the tension torsion machine. There is obviously a drift in the internal displacement sensor of the test machine during the characterization steps depending on the fatigue loads. Apart from the steps between both parts of the slopes the typical behaviour of a slow linear decrease of the Young's Modulus and the Shear Modulus after the rapid decrease at the beginning and until the final failure is visible.

The relationship between the loading and the stiffness degradation is linked to the crack development of each ply. As stated already, for this reason the cracks were counted for each layer and in figure 5 the crack density δ versus the life cycles is plotted for the same specimen as shown in figure 4. Under pure shear load the crack density in all layers increases slowly, but under pure tension load a very rapid increase of crack density in $\pm 45^\circ$ - and 90° -direction are determined. In this phase the cracks under 0° develop slowly further on. The main reason for this behaviour is the intralaminar loading of the $\pm 45^\circ$ - and 90° -layers under tension load, while the tension load has no influence on the crack density of 0° -orientation. During the second shear loading block the crack density of the $\pm 45^\circ$ - and 90° -layers shows saturation and

the cracks in 0°-direction increase fast as a result of load transfer between the -45°- and the 0°- layers.

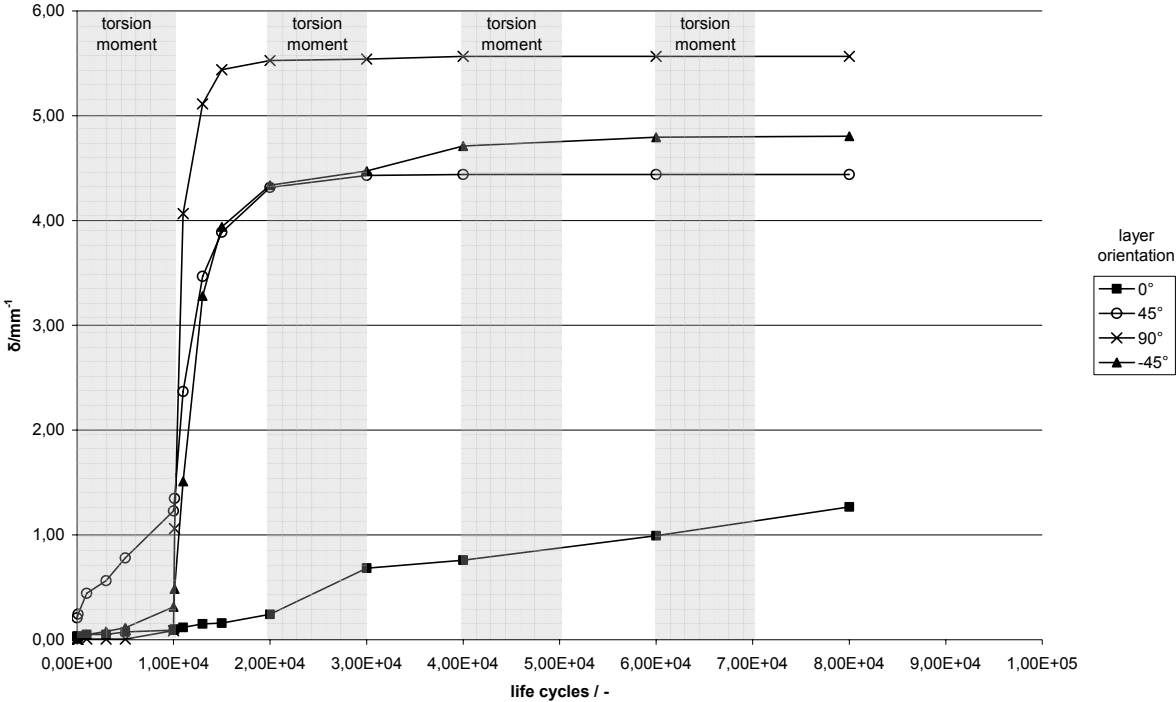


Figure 5: Crack densities of different orientation for a specimen under sequence fatigue shear and compressive/tension load

The important fact is the relationship of the stiffness degradation and the increase of the crack density. The stiffness degradation shown in figure 4 appears with the rapid increase of crack density in the most layers. Gagel et al. [7] and Adden et al. [5] showed comparable behaviours for specimens under pure compressive/tension and pure shear loads. Under pure compressive/tension the crack densities of the different layers show a very rapid increase during the first life cycles (10 – 15 % of life) and a saturation until the final failure. This is comparable to the first compressive/tension loading block shown in figure 5. The maximum values of the crack densities are also comparable to experiments under pure compressive/tension loads. The crack densities under pure shear loads increase more slowly and saturation could not be measured as under pure compressive/tension loads. The same behaviour at the beginning under pure shear loads can also be observed in the first shear loading block in the current experimental tests. These experiments and the current work show the relationship of the stiffness degradation and crack density and is therefore the base of the modelling approach.

Figure 6 shows the experimental results of one further specimen using a changed load sequence. The first loading block (until 10000 life cycles and 10 – 15 % of life) was compressive/tension load. One observes a rapid decrease of the Young’s Modulus during the first 5000 life cycles and after 80000 life cycles (approximately 90% of the life). The last rapid decrease ends in the final failure of the specimen. Between these two phases a slow linear decrease is measured. A similar behaviour is visible for the Shear Modulus. Figure 6 also shows that the rapid stiffness degradation appears under pure compressive/tension load and this is also comparable to the experiments under pure compressive/tension loads shown by Adden et al. [5].

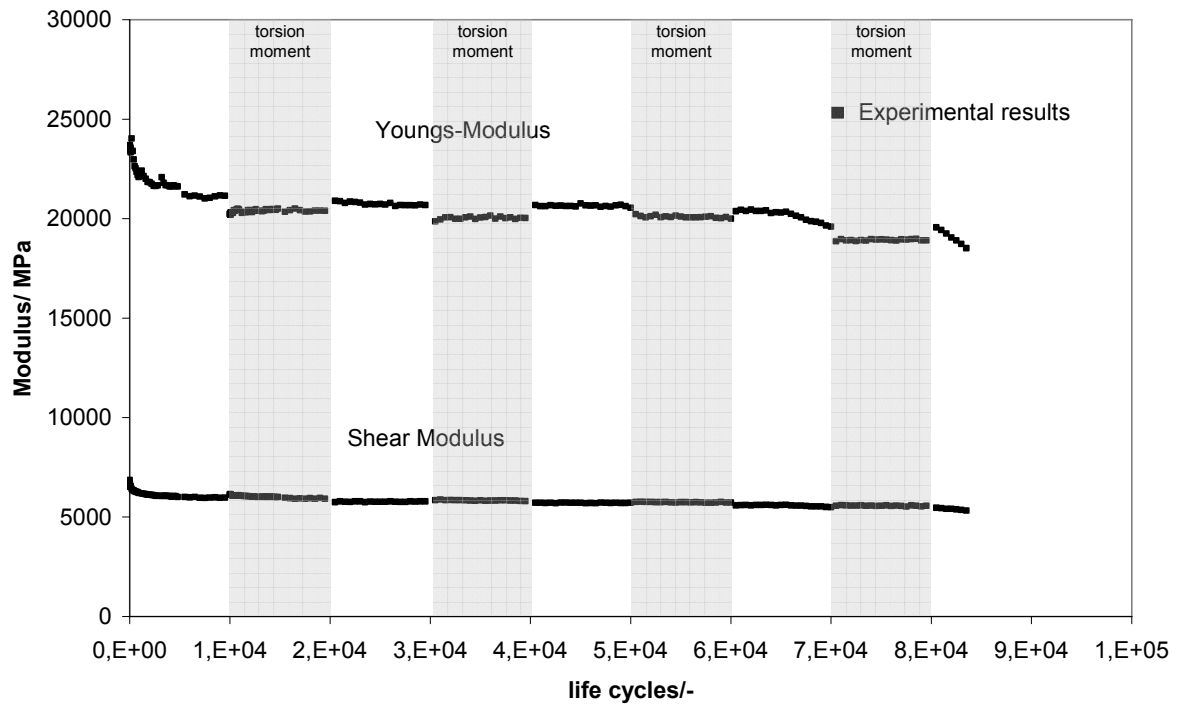


Figure 6: Experimental degradation results of Young's and Shear Modulus for a specimen under sequence fatigue compressive/tension and shear load

5. COMPARISON BETWEEN MODEL PREDICTIONS AND EXPERIMENTS

For a comparison between the modelling approach and the experimental results the crack densities measured during the experiments with the NCFs were included into the model. On account of this it is necessary to compute the stiffness of all plies in the NCF. According to the crack densities of the experiments each ply was degraded and the unidirectional-coordinate system was transformed into the global coordinate system. So the total stiffness matrix of the NCF was calculated. An example of the comparison of model and experiments (the same specimen shown in figure 4) depicts figure 7. One can observe that the model shows a similar slope for the Young's and Shear Modulus. Because of the linking of crack density and stiffness degradation and the implementation into the model the slow linear decrease during the first shear loading block is captured quite well. The decrease of the stiffness as a result of the increase of the crack density under pure compressive/tension load and the following linear decrease until final failure is also shown very well. By looking at the overall behaviour of the stiffness degradation the deviation between the model and the measured stiffness degradation regarding the Young's Modulus is clearly visible. As mentioned above, the Young's Modulus can be calculated by using the stresses and strains from the characterization steps. In order to prevent cracks caused by the normal stress into the characterization step the normal stress amplitude were quite small. The strains were calculated by using the internal displacement sensor of the test machine. The combination of small stress and high stiffness of the specimen causes very small displacements in axial direction. This leads to a very bad signal compared to the internal displacement sensor range. For the circumferential direction this is no problem, because the displacements under the shear loads are high enough. Adden et al. [6] also show this effect and table 2 visualizes that the Shear Modulus is continuously computed very well with a maximum deviation of approximately 5 %.

		Young's Modulus / MPa	Shear Modulus / MPa
Static experiment	Strain gauge	28580	6617
At the beginning	Internal Sensor	25293	7329
	Modelling approach	25702	6971
After 10000 life cycles	Internal Sensor	24771	6725
	Modelling approach	25233	6826
After 20000 life cycles	Internal Sensor	22016	6411
	Modelling approach	23261	6414

Table 2: Stiffness degradation of a tube specimen compared to the modelling approach

Furthermore one can observe that the internal displacement sensor leads to a much lower Young's Modulus compared to the measurements with strain gauges. The problem is that strain gauges could not be used during fatigue experiments because due to high fatigue loads they failed after a few hundred cycles. This is certainly a problem which will be followed and solved in further works. The positive result of the Shear Modulus and the reproduction of the overall behaviour of the stiffness degradation show that the model is capable for the application by NCFs and under sequence loads.

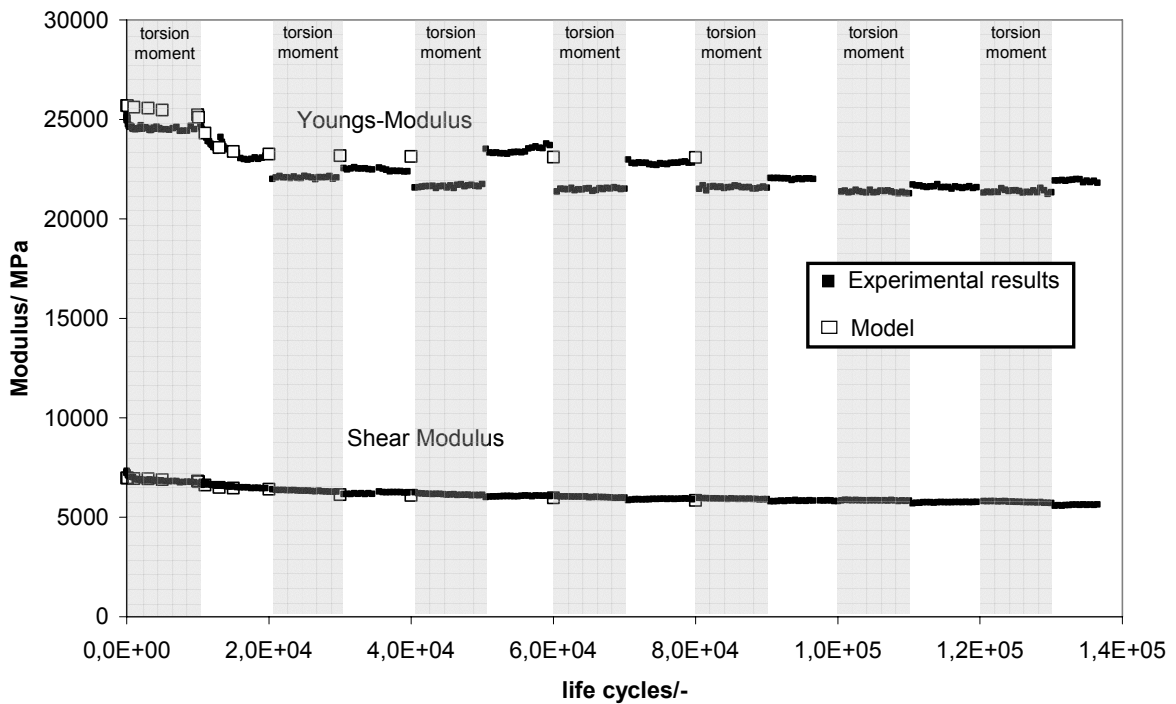


Figure 7: Experimental degradation results of Young's and Shear Modulus compared to the model for a specimen under sequence fatigue shear and compressive/tension load

6. CONCLUSIONS

The procedures and results of sequence fatigue loaded NCFs are presented and the applicability of a model is shown by using the experimental results. For each specimen the crack densities were taken, the stiffness degradation was modelled and the total stiffness of the specimen was calculated by using classical laminate theory. These results are compared to the stiffness degradation in axial direction (Young's Modulus) and in torsional direction (Shear Modulus). The overall prediction of the model is very good. The model allows to calculate ply-stresses for a given damage state, which will help to establish damage accumulation criteria for sequence loaded NCFs.

ACKNOWLEDGEMENTS

The authors wish to thank SAERTEX^R for supplying the NCFs and the German Research Foundation (DFG) for funding this research.

REFERENCES

- 1- Bibo G.A., Hogg P.J., Kemp M., "Mechanical characterisation of glass- and carbon-fibre-reinforced composites made with non-crimps fabrics", *Composite Science and Technology*, 1997, Vol. 57, pp. 1221-1241,
- 2- Hogg P.J., Ahmadnia A., Guild F.J., "The mechanical properties of non-crimped fabric-based composites", *Composites*, 1995, Vol. 24, No. 5, pp. 423-432
- 3- Carvelli V., Corigliano A., "Transversal resistance of long-fibre composites: Influence of the fibre-matrix interface", *Proceeding of the 11 ECCM*, 2004, Rhodes, Greece
- 4- Carvelli V., Chi T., Larosa M., Lomov S., Poggi C., Angulo D., Verpoest I., "Experimental and numerical determination of the mechanical properties of multi-axial multi-ply composites", *Proceeding of the 11 ECCM*, 2004, Rhodes, Greece
- 5- Adden S., Horst P., "Damage propagation in non-crimp fabrics under bi-axial static and fatigue loading", *Composite Science and Technology*, 2006, Vol. 66, pp. 626-633
- 6- Adden S., Horst P., "Stiffness degradation under fatigue in multiaxially loaded non-crimped fabrics", submitted to *Journal of fatigue*, 2008
- 7- Gagel A., Müller C., Schulte K., "On the damage evolution and the mechanical degradation of glass-fiber non crimp-fabric reinforced epoxy under tensile loading: Experimental and finite element modelling", *Multidiscipline modelling in materials and structures*, 2006, Vol. 2(1), pp. 117-126